Supporting Information File

Proton Conduction in a Hydrogen-Bonded Complex of Copper(II)-Bipyridine Glycoluril Nitrate

Sakharam B. Tayade,[a] Vishal M. Dhavale,[b,c] Avinash S. Kumbhar,[*,a] Sreekumar Kurungot,[b,c] Peter Lönnecke,[d] Evamarie Hey-Hawkins,[d] and Bhalchandra Pujari[e]

[a]Department of Chemistry, Savitribai Phule Pune University, Pune- 411007, India.
E-mail: askum@chem.unipune.ac.in
[b]Physical & Materials Chemistry Division, National Chemical Laboratory, Pune- 411007, India.
[c]Academy of Scientific and Innovative Research (AcSIR), Anusandhan Bhavan, 2 Rafi Marg, New Delhi-110 001, India.
[d]Faculty of Chemistry and Mineralogy, Institute of Inorganic Chemistry, Universität Leipzig, Johannisallee 29, 04103, Leipzig, Germany.
[e]Centre for Modeling and Simulation, Savitribai Phule Pune University, Pune-411007, India.

CONTENT

Section I: Experimental

1a) Synthesis of bipyridine glycoluril (BPG): Condensation of 1,10-phenanthroline-5,6-dione (0.5 g, 2.38 mmol) and urea (0.35 g, 5.83 mmol) in methanol with trifluoroacetic acid (2.71 g, 23.78 mmol) yielded 60% of BPG, as an insoluble white powder, which was isolated, washed with water and diethyl ether, and then dried in vacuum.
Yield: 60 %; elemental analysis calcd. for $C_{14}H_{10}N_6O_2 \cdot 2H_2O$: C, 50.86; H, 4.27; N, 25.44%; Found: C, 51.54; H, 4.33; N, 25.75%; ^{1}H NMR (DMSO-d_6, room temperature, ppm): δ = 8.72 (d, 2H), 8.31 (s, 4H), 8.06 (d, H), 7.54 (dd, 2H); I.R. (KBr, cm^{-1}): C=O (1695), N-H (3209), O-H (3418), C=N (1581), C=C (1450); mp >330 °C.

1b) Synthesis of $[Cu(BPG)_2(H_2O)](NO_3)_2 \cdot 4H_2O$ (1): This complex was prepared by the 1:2 reaction of $Cu(NO_3)_2 \cdot 3H_2O$ (82.1 mg, 0.33 mmol) and BPG (200 mg, 0.67 mmol) in 1:1 methanol-water at reflux for 12 h whereupon the color of the solution changed to dark green. The resulting solution was cooled to room temperature and filtered. The solvent was evaporated and the crude product purified by column chromatography on active alumina using methanol and water as an eluent. Single crystals were grown by slow evaporation of a methanol-water solution.
Yield: 75%; elemental analysis calcd. for $C_{28}H_{30}CuN_{14}O_{15}$: C, 38.83; H, 3.49; N, 22.64 %. Found: C, 38.21; H, 3.12; N, 22.46 %.

Section II: IR Spectroscopy of Compound **1**

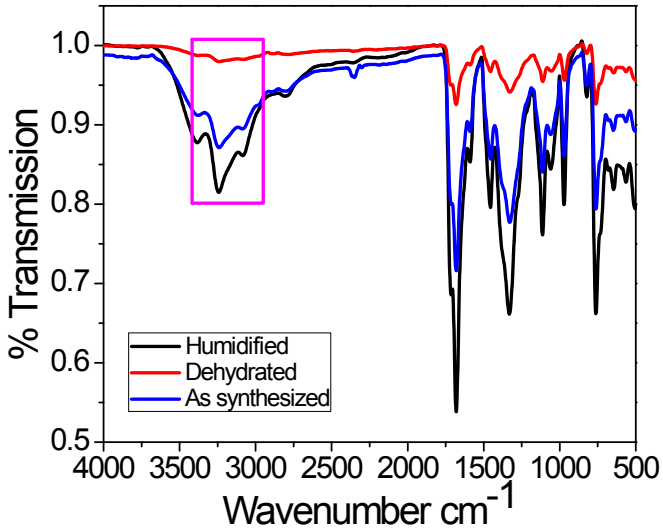

Figure S1. IR spectra showing reversible hydration and dehydration of **1**.

Section III: X-Ray Crystallographic Data and Refinement Parameters for Compound **1**

Molecular Formula	$[Cu(BPG)_2(H_2O)](NO_3)_2 \cdot 4H_2O$
Empirical formula	$C_{28}H_{30}CuN_{14}O_{15}$
Formula weight	866.20
Temperature	293(2) K
Wavelength	71.073 pm
Crystal system	Tetragonal
Space group	P 4_2/n b c
Unit cell dimensions	a = 1633.57(2) pm α = 90° b = 1633.57(2) pm β = 90° c = 1295.57(4) pm γ = 90°
Volume	3.4573(1) nm^3
Z	4
Density (calculated)	1.664 Mg/m^3
Absorption coefficient	0.727 mm^{-1}
F(000)	1780
Crystal size	0.4 x 0.4 x 0.2 mm^3
Theta range for data collection	2.494 to 26.365°.
Index ranges	-20 <=h <=11, -14 <=k <=20, -16 <=l <=15
Reflections collected	10630
Independent reflections	1778 [R(int) = 0.0367]
Completeness to theta = 26.365°	99.9 %
Absorption correction	Semi-empirical from equivalents
Max. and min. transmission	1 and 0.98852
Refinement method	Full-matrix least-squares on F^2
Data / restraints / parameters	1778 / 29 / 148
Goodness-of-fit on F^2	1.067
Final R indices [I>2sigma(I)]	R1 = 0.0595, wR2 = 0.1662
R indices (all data)	R1 = 0.0800, wR2 = 0.1836
Residual electron density	0.291 and -0.435 e. $Å^{-3}$

Table S1. Atomic coordinates (x 10^4) and equivalent isotropic displacement parameters (pm^2 x 10^{-1}) for compound **1**. U(eq) is defined as one third of the trace of the orthogonalized U_{ij} tensor.

	x	y	z	U(eq)
Cu(1)	2500	2500	5423(1)	52(1)
O(1)	1402(2)	6797(2)	6745(2)	61(1)
O(2)	2500	2500	7086(6)	91(3)
O(6)	425(2)	8103(2)	6170(3)	76(1)
N(1)	3251(2)	3409(2)	5351(3)	68(1)
N(2)	2519(2)	6003(2)	6313(2)	43(1)
N(3)	1578(2)	6243(2)	5137(2)	44(1)
C(1)	2908(2)	4155(2)	5237(3)	46(1)
C(2)	3284(2)	4863(2)	5540(2)	39(1)
C(3)	4054(2)	4806(2)	6003(2)	50(1)
C(4)	4403(2)	4047(2)	6123(3)	62(1)
C(5)	3988(2)	3362(2)	5792(4)	75(1)
C(6)	2875(2)	5681(2)	5379(2)	35(1)
C(7)	1797(2)	6392(2)	6124(2)	44(1)
O(3)	-907(6)	8211(6)	7698(9)	138(3)
O(4)	-565(5)	9435(5)	7500	146(5)
N(4)	-1066(5)	8934(5)	7500	72(2)
O(3F)	-1132(13)	8422(9)	6710(15)	138(3)
O(4F)	-844(9)	9647(8)	7033(11)	98(4)
O(5F)	-1795(11)	9049(13)	7797(16)	138(3)
N(4F)	-1228(8)	9062(9)	7145(10)	72(2)

Table S2. Bond lengths [pm] and angles [°] for compound **1**

Cu(1)-Cu(1)#1	109.6(2)
Cu(1)-N(1)	192.8(3)
Cu(1)-N(1)#2	192.8(3)
Cu(1)-O(2)	215.5(8)
Cu(1)-N(1)#3	217.1(3)
Cu(1)-N(1)#1	217.1(3)
O(1)-C(7)	122.5(4)
N(1)-C(5)	133.5(5)
N(1)-C(1)	134.9(4)

N(1)-Cu(1)#1	217.1(3)
N(2)-C(7)	136.2(4)
N(2)-C(6)	144.2(3)
N(3)-C(7)	135.0(4)
N(3)-C(6)#1	144.4(4)
C(1)-C(2)	136.7(4)
C(1)-C(1)#1	146.8(6)
C(2)-C(3)	139.6(4)
C(2)-C(6)	151.0(4)
C(3)-C(4)	137.4(5)
C(4)-C(5)	137.7(6)
C(6)-N(3)#1	144.4(4)
C(6)-C(6)#1	157.1(5)
Cu(1)#1-Cu(1)-N(1)	87.2(1)
Cu(1)#1-Cu(1)-N(1)#2	87.2(1)
N(1)-Cu(1)-N(1)#2	174.4(2)
Cu(1)#1-Cu(1)-O(2)	180.0
N(1)-Cu(1)-O(2)	92.8(1)
N(1)#2-Cu(1)-O(2)	92.8(1)
Cu(1)#1-Cu(1)-N(1)#3	62.5(1)
N(1)-Cu(1)-N(1)#3	98.4(2)
N(1)#2-Cu(1)-N(1)#3	79.04(2)
O(2)-Cu(1)-N(1)#3	117.5(1)
Cu(1)#1-Cu(1)-N(1)#1	62.5(1)
N(1)-Cu(1)-N(1)#1	79.04(2)
N(1)#2-Cu(1)-N(1)#1	98.4(2)
O(2)-Cu(1)-N(1)#1	117.5(1)
N(1)#3-Cu(1)-N(1)#1	125.0(2)
C(5)-N(1)-C(1)	118.2(3)
C(5)-N(1)-Cu(1)	120.6(3)
C(1)-N(1)-Cu(1)	115.9(2)
C(5)-N(1)-Cu(1)#1	131.9(3)
C(1)-N(1)-Cu(1)#1	109.5(2)
Cu(1)-N(1)-Cu(1)#1	30.28(8)
C(7)-N(2)-C(6)	111.6(2)
C(7)-N(3)-C(6)#1	112.9(2)
N(1)-C(1)-C(2)	123.1(3)
N(1)-C(1)-C(1)#1	115.04(2)
C(2)-C(1)-C(1)#1	121.9(2)
C(1)-C(2)-C(3)	118.2(3)
C(1)-C(2)-C(6)	120.7(3)
C(3)-C(2)-C(6)	121.1(3)
C(4)-C(3)-C(2)	118.9(3)
C(3)-C(4)-C(5)	119.5(3)
N(1)-C(5)-C(4)	122.1(3)
N(2)-C(6)-N(3)#1	114.0(2)
N(2)-C(6)-C(2)	112.6(2)
N(3)#1-C(6)-C(2)	110.7(2)
N(2)-C(6)-C(6)#1	102.1(3)
N(3)#1-C(6)-C(6)#1	101.1(2)
C(2)-C(6)-C(6)#1	115.6(2)
O(1)-C(7)-N(3)	125.4(3)
O(1)-C(7)-N(2)	126.2(3)
N(3)-C(7)-N(2)	108.4(2)

Symmetry transformations used to generate equivalent atoms:

#1 -x+1/2,y,-z+1 #2 -x+1/2,-y+1/2,z #3 x,-y+1/2,-z+1

#4 y-1,x+1,-z+3/2

Table S3. Anisotropic displacement parameters (pm^2 x 10^{-1}) for compound **1**. The anisotropic displacement factor exponent takes the form: $-2\pi^2 [h^2 a^{*2} U_{11} + ... + 2 h k a^* b^* U_{12}]$

	U^{11}	U^{22}	U^{33}	U^{23}	U^{13}	U^{12}
Cu(1)	42(1)	31(1)	83(1)	0	0	1(1)
O(1)	69(2)	64(2)	50(1)	-18(1)	0(1)	19(1)
O(2)	84(6)	115(8)	74(5)	0	0	-10(5)
O(6)	59(2)	67(2)	101(2)	18(2)	16(2)	3(2)
N(1)	39(2)	36(2)	130(3)	8(2)	5(2)	4(1)
N(2)	49(2)	47(1)	32(1)	-4(1)	-5(1)	8(1)
N(3)	43(1)	45(1)	44(1)	-8(1)	-8(1)	10(1)
C(1)	34(2)	33(2)	71(2)	4(1)	6(1)	4(1)
C(2)	36(2)	40(2)	43(2)	5(1)	2(1)	3(1)
C(3)	44(2)	50(2)	55(2)	1(2)	-6(1)	5(2)
C(4)	43(2)	64(2)	78(2)	10(2)	-9(2)	14(2)
C(5)	48(2)	49(2)	127(4)	18(2)	5(2)	14(2)
C(6)	35(2)	34(1)	35(1)	1(1)	-2(1)	-1(1)
C(7)	49(2)	39(2)	44(2)	-4(1)	0(1)	1(1)

Table S4. Hydrogen bonds for compound **1** [pm and °].

D-H···A	d(D-H)	d(H···A)	d(D···A)	<(DHA)
N(2)-H(1N2)···O(1)#5	86	203	282.9(3)	153.8
N(3)-H(1N3)···O(6)#6	86	192	274.9(4)	162.4
O(2)-H(1O2)···O(3)#7	96	204	296.(1)	158.9
O(2)-H(2O2)···O(3)#8	96	195	286(1)	158.7
O(2)-H(1O2)···O(3)#5	96	247	286(1)	104.5
O(2)-H(2O2)···O(3)#9	96	236	296.(1)	120.3
O(6)-H(1O6)···O(1)	96(2)	180(2)	276.7(4)	177(4)
O(6)-H(2O6)···O(3)	95(2)	212(4)	295(1)	146(5)

Symmetry transformations used to generate equivalent atoms:

#1 -x+1/2,y,-z+1 #2 -x+1/2,-y+1/2,z #3 x,-y+1/2,-z+1

#4 y-1,x+1,-z+3/2 #5 -y+1,x+1/2,-z+3/2 #6 x,-y+3/2,-z+1

#7 -x,y-1/2,z #8 y-1/2,-x,-z+3/2 #9 x+1/2,-y+1,z

Section IV: Packing diagrams of Compound **1**

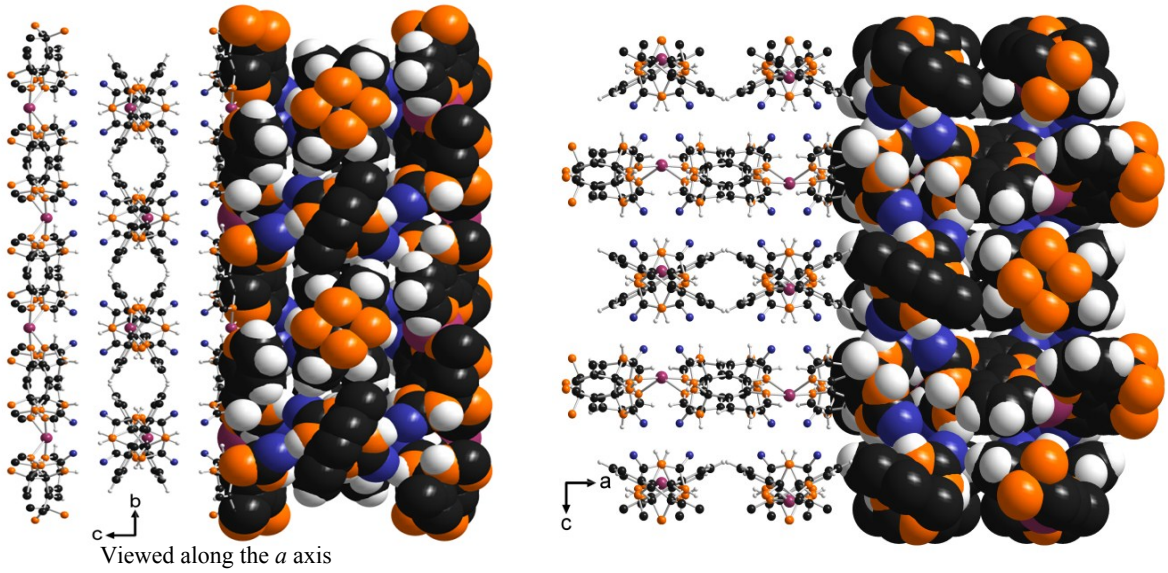

Viewed along the *a* axis Viewed along the *b* axis

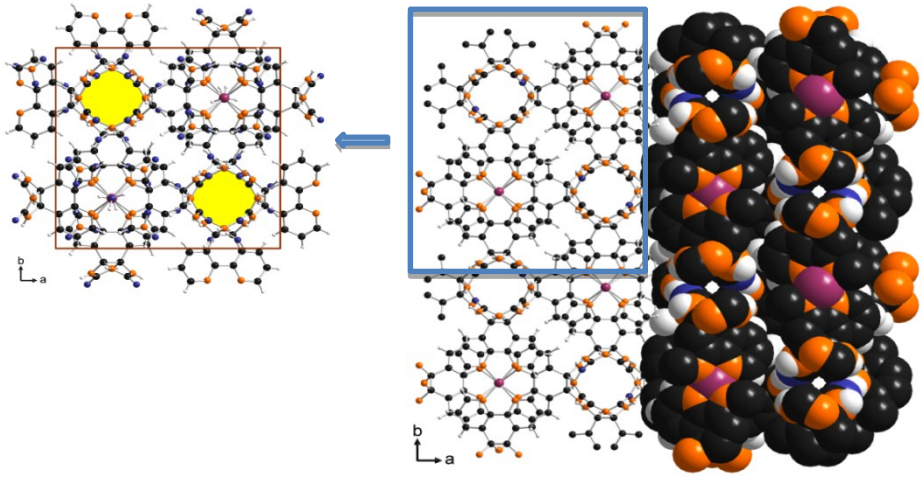

Viewed along the *c* axis

Figure S2. Packing diagram of compound **1** viewed along the *a*-, *b*- and *c*-axis in ball-and-stick and space-filling presentation. To visualize possible ion conductive channel, nitrate anions, water molecules and disordered copper atoms are omitted. The small channels along *c* (100×100 pm) highlighted in yellow are not occupied.

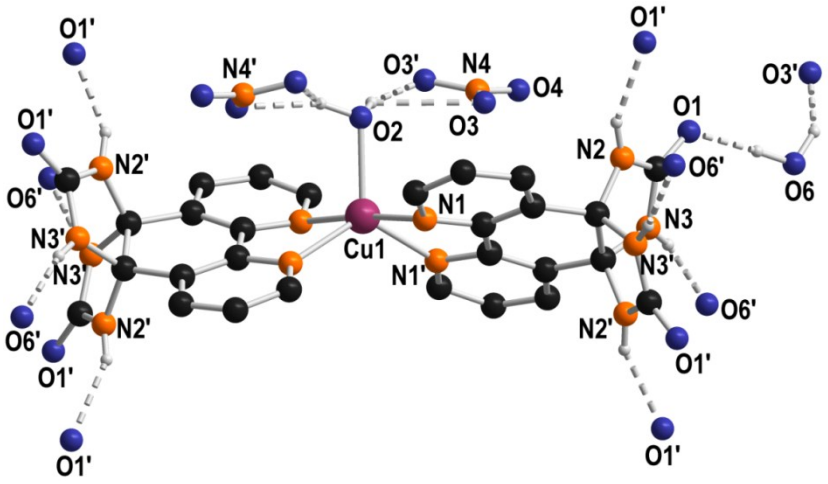

Figure S3. Intermolecular hydrogen donor-acceptor bonds. The nitrate anion is found to be highly disordered on a twofold axis. For this reason it could be located only with reduced accuracy. Atoms labelled with dash are symmetry generated [Symmetry operators to generate equivalent atoms: (‘): 0.5-x, y, 1-z; (’’): x, 0.5-y, 1-z; (’’’): 0.5-x, 0.5-y, z)]. For intermolecular hydrogen donor-acceptor bonds see also Table S4.

Section V: Thermal Stability of Compound **1**

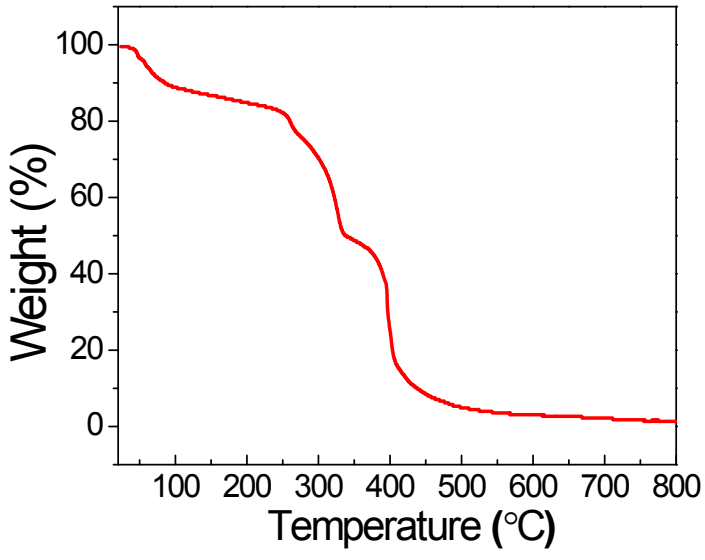

Figure S4. TGA Profile of compound **1** showing weight loss with increase in temperature.

Section VI: Proton Conductivity of Compound **1**

For the impedance analysis, pellet size 1.3 cm in diameter and 0.085 cm in thickness has been used. The proton conductivity of pelletized compound **1** was determined by using the following equation;

$$\sigma = l / (R \times A)$$

Where, σ = proton conductivity (Scm^{-1}), l = pellet thickness (cm), R = resistance of the pellet (Ω) and A = area of the pellet (cm^2).

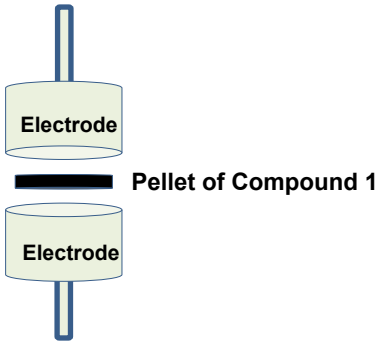

Figure S5. Illustration of sandwiched pellet between two stainless steel electrodes.

The resistance values of the pellet were determined from the fitting model, shown below:

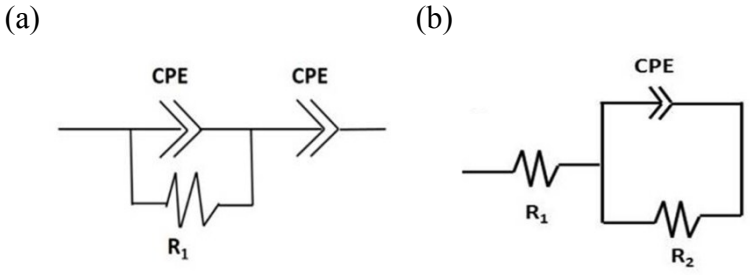

The equivalent circuit (a) has been used for fitting the Nyquist plot measured at 40 and 50% RH by keeping temperature constant (90 °C), and equivalent circuit (b) is used for all other remaining Nyquist plots.
Here, CPE is the Constant Phase Element, R1 is the resistance of conduction (used for calculation), and R2 is the charge transfer resistance. For better circuit fitting, the fitting has been done after removing inductance part.

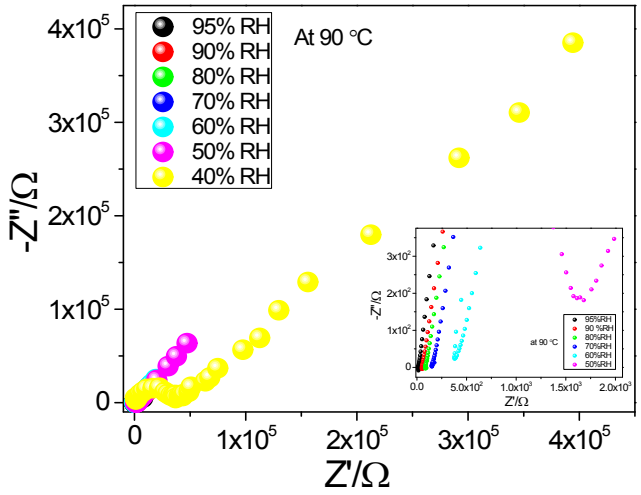

Figure S6. Nyquist plot of compound **1** at different %RH showing increase in proton conductivity.

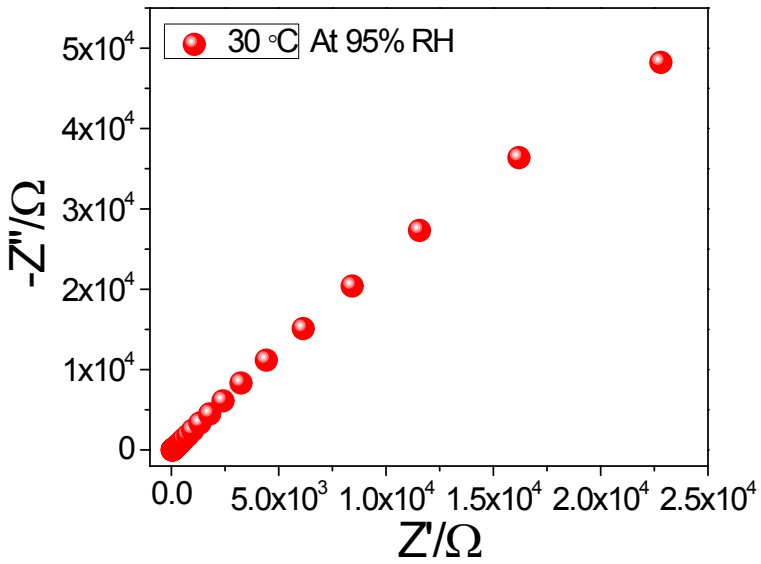

Figure S7. Nyquist plot of compound **1** showing lowest conductivity at T = 30 °C and 95% RH.

Table S6 A: Comparison of proton conductivity of Compound **1** with other complexes

Complex	Proton Conductivity [Scm^{-1}]	Temperature [°C]	Humidity (RH) [%]	Reference
$[Co(H_2bim)_3]^{3+}$. $TATC^{3-}$ H_2bim = 2,2′-biimidazole $TATC^{3-}$ = 1,3,5-tricarboxyl-2,4,6-triazinate	10^{-5}	26.8	saturated water vapor	1
$Co[Cr(CN)_6]_{2/3\cdot Z}H_2O$	1.2×10^{-3} 1.7×10^{-3}	20 35	100 100	2
$V[Cr(CN)_6]_{2/3\cdot Z}H_2O$	1.6×10^{-3} 2.6×10^{-3}	20 50	100 100	2
$Cu_3(L)_2(H_2O)_4[Cu(dmf)_4(SiW_{12}O_{40})]\cdot 9H_2O$ L = L{*N*,*N*′-bis[(2-hydroxy-3-methoxyphenyl) methylidene]hydrazine hydrate}	10^{-4}	100	98	3
$[Cu(BPG)_2(H_2O)](NO_3)_2$	**4.45×10^{-3}**	**90**	**95**	**Present Work**

Table S5 B: Comparison of proton conductivity of Compound **1** with Hydrogen-Bonded Frameworks (HOFs)

Hydrogen-Bonded Framework (HOF)	Proton Conductivity [Scm^{-1}]	Temperature [°C]	Humidity (RH) [%]	Reference
HOF-GS-10 [(1,5-Naphthalenedisulfonate)(guanidinium)$_2$]·xG HOF-GS-11 [(4,4'-Biphenyl sulfonate (guanidinium)$_2$]·xG	0.75×10^{-2} Scm^{-1} 1.8×10^{-2} Scm^{-1}	30	95	4
HOF-6 Diaminotriazine-Decorated Porphyrin HOF	3.4×10^{-6} Scm^{-1}	27	97	5
cucurbit[6]uril	1.3×10^{-3} Scm^{-1}	25	98	6

Table S5 C: Comparison of proton conductivity of Compound **1** with MOFs/PCPs

MOFs/PCPs	Proton Conductivity [Scm^{-1}]	Temperature [°C]	Humidity (RH) [%]	Reference
$\{Fe(ox)(H_2O)_2\}$ (ox = $C_2O_4^{2-}$)	1.3×10^{-3}	25	98	7

$[Cu(bpdc)(H_2O)]_n$ H_2bpdc = 2,2′-bipyridyl-3,3′-dicarboxylic acid	1.55×10^{-4}	100	98	8
$\{Mn(DHBQ)(H_2O)_2\}$ DHBQ = 2, 5-dihydroxy-1, 4-benzoquinone	4×10^{-5}	25	98	9
$\{[M_3(HL)_3(H_2O)_6]n.13n(H_2O)\}$ [Fe^{II} (**1**), Co^{II} (**2**)] H_3L = oxonic acid	1.3×10^{-6} (**1**) 1.2×10^{-4} (**2**)	80º	95	10
$(NH_4)_2(adp)[Zn_2(ox)_3].3H_2O$ ox = oxalate adp = adipic acid	8×10^{-3}	25	98	11
$MgH_6ODTMP.6H_2O$ H_6ODTMP = octamethylenediamine-N,N,N′,N′ tetrakis(methylenephosphonic acid)	1.6×10^{-3}	19	100	12
$La(H_5DTMP).7H_2O$ H_8DTMP, hexamethylenediamine-N,N,N′,N′-tetrakis(methylenephosphonic acid)	8×10^{-3}	24	98	13

Section VII: PXRD Pattern of Compound **1** Before and After Impedance Measurement

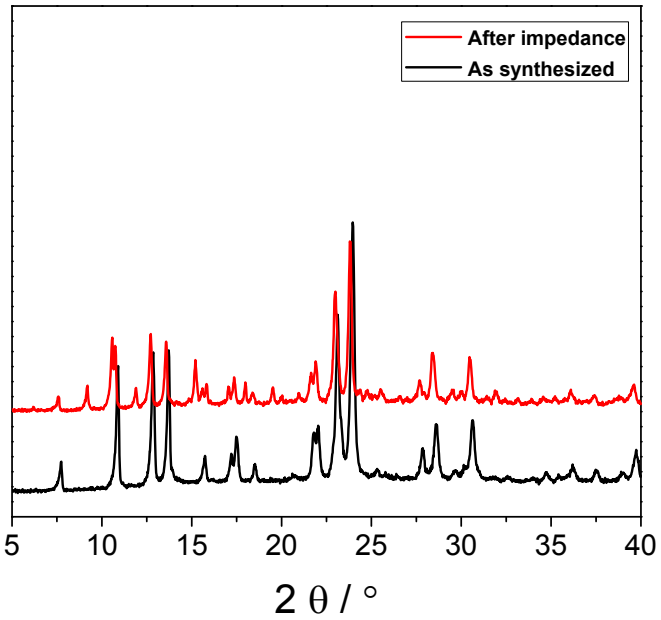

Figure S8. PXRD Pattern of Compound **1** before and after Impedance measurement showing that the structure remains intact after measurement.

Section VIII: Theoretical investigations

Density functional theory-based *ab-initio* calculations were performed using the Perdew-Burke-Ernzerhof exchange correlations functional[14,15] as implemented in the Quantum ESPRESSO package. The molecule is isolated from its periodic images using 12 Å of vacuum in all three

directions. The kinetic energy cutoff for plane-wave basis was kept to 950 eV. First, unconstrained relaxation of the Cu complex with and without water molecule was performed. Figures S9 and S10 show the effects of water molecules on the Highest Occupied Molecular Orbital (HOMO) and the Lowest Unoccupied Molecular Orbital (LUMO). Isosurfaces of charge densities are plotted for the HOMO and LUMO with and without water molecule. Clearly, in the absence of water the orbitals are *p* and *d* dominated, while the water distorts both of them resulting in strong hybridized orbitals. Yet, there is no charge density on the water molecule itself. The binding energy of the water was found to be 0.085 eV.

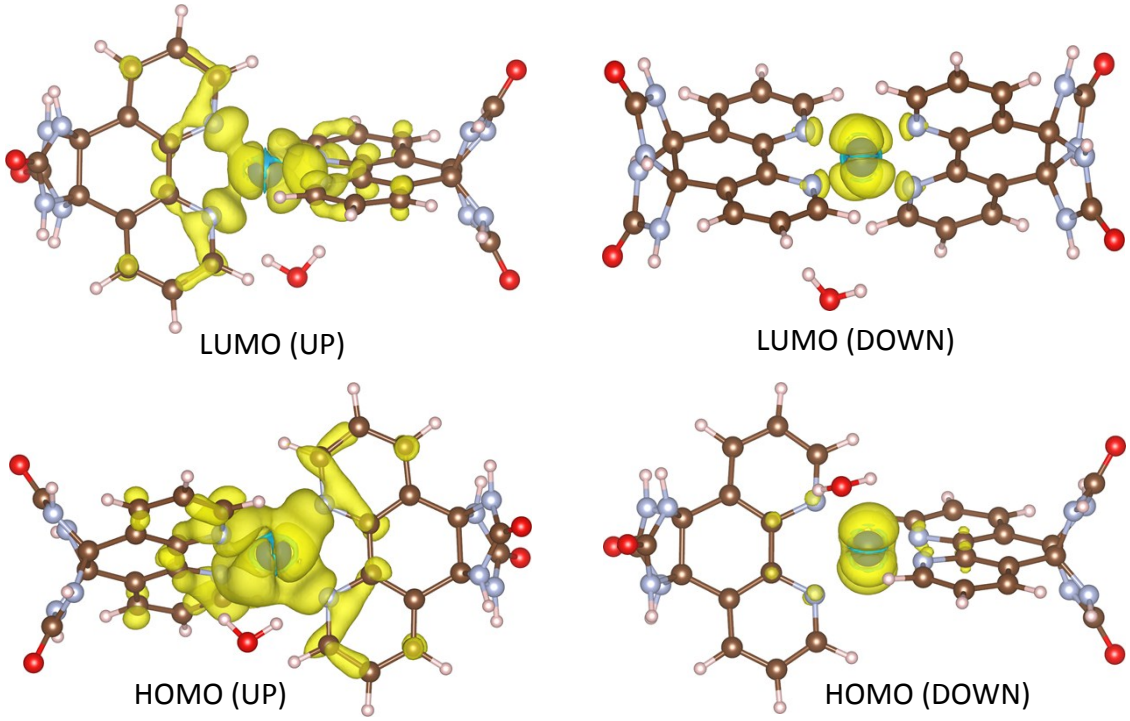

Figure S9. Isosurfaces of charge densities of HOMO and LUMO orbitals of the two spin channels of the Cu Complex without a water molecule.

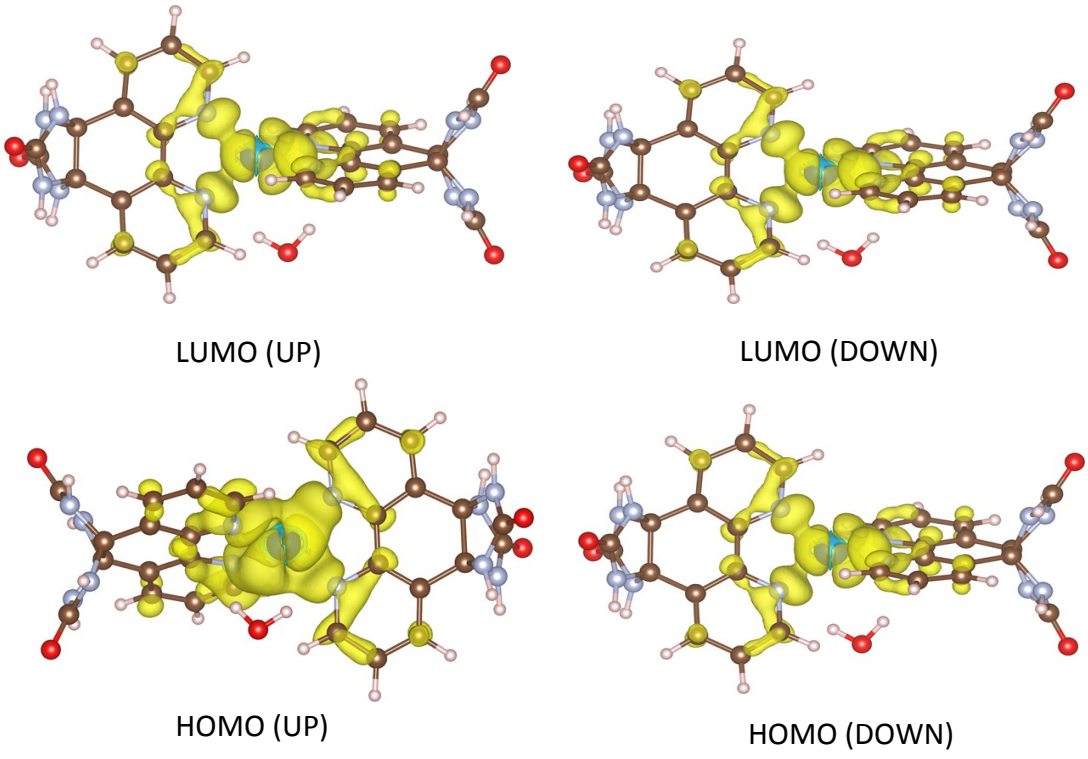

Figure S10. Isosurfaces of charge densities of HOMO and LUMO orbitals of two spin channels in the presence of a water molecule.

Molecular dynamics (MD) calculations were performed within the Born-Oppenheimer approximations at 350 K for 2.8 ps at a time step of 2.4 fs. This was sufficient to confirm the conjecture of a proton hopping mechanism. In order to simulate the humidity, up to twelve water molecules were placed in the vicinity of the Cu complex. Figure S11 shows three snapshots of MD simulations. The temperature-induced distortions of the molecule are seen as expected. The frames are chosen such that the hopping of H^+ is clearly evident. The hopping is observed in as small as 300 fs duration thus the total duration of MD, although small, is sufficient to establish the hopping mechanism. It would be a very compute intensive job to determine the reaction pathways using only MD. Hence taking the input from the MD calculations we performed the Climbing Image Nudged Elastic Band calculations as explained in the main text.

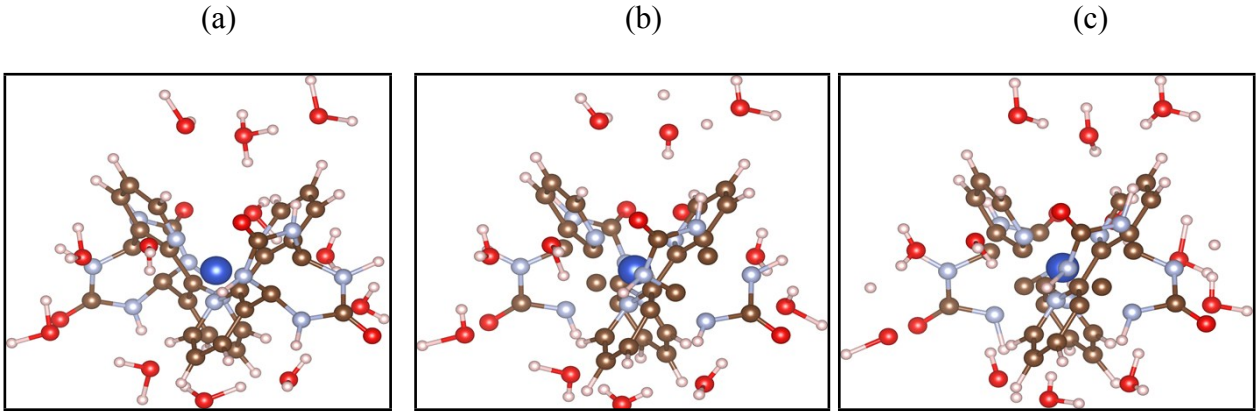

Figure S11. Snapshots from MD simulations taken at 0 fs, 268 fs, and 300 fs. Notice that the H_3O^+ molecule at the center top of figure (a) loses its proton (b) at about 268 fs which then hops to the water molecule in the top left corner in figure (c). Elongated bond lengths are the results of finite temperature vibrations.

REFERENCES

1. M. Tadokoro, Y. Ohhata, Y. Shimazaki, S. i. Ishimaru, T. Yamada, Y. Nagao, T. Sugaya, K. Isoda, Y. Suzuki and H. Kitagawa, *Chem. Eur. J.*, 2014, **20**, 13698-13709.
2. S.-i. Ohkoshi, K. Nakagawa, K. Tomono, K. Imoto, Y. Tsunobuchi and H. Tokoro, *J. Am. Chem. Soc.*, 2010, **132**, 6620-6621.
3. M. L. Wei, J. J. Sun and X. Y. Duan, *Eur. J. Inorg. Chem.*, 2014, **2014**, 345-351.
4. A. Karmakar, R. Illathvalappil, B. Anothumakkool, A. Sen, P. Samanta, A. V. Desai, S. Kurungot and S. K. Ghosh, *Angew. Chem. Int. Ed.*, 2016, **55**, 1-6.
5. W. Yang, F. Yang, T.-L. Hu, S. C. King, H. Wang, H. Wu, W. Zhou, J.-R. Li, H. D. Arman and B. Chen, *Cryst. Growth Des.*, 2016.
6. M. Yoon, K. Suh, H. Kim, Y. Kim, N. Selvapalam and K. Kim, *Angew. Chem. Int. Ed.*, 2011, **50**, 7870-7873.
7. T. Yamada, M. Sadakiyo and H. Kitagawa, *J. Am. Chem. Soc.*, 2009, **131**, 3144-3145.
8. M. Wei, X. Wang and X. Duan, *Chem. Eur. J.*, 2013, **19**, 1607-1616.
9. S. Morikawa, T. Yamada and H. Kitagawa, *Chem. Lett.*, 2009, **38**, 654-655.
10. S. Goswami, S. Biswas and S. Konar, *Dalton Trans.*, 2015, **44**, 3949-3953.
11. R. M. Colodrero, P. Olivera-Pastor, E. R. Losilla, D. Hernández-Alonso, M. A. Aranda, L. Leon-Reina, J. Rius, K. D. Demadis, B. Moreau and D. Villemin, *Inorg. Chem.*, 2012, **51**, 7689-7698.
12. R. M. Colodrero, P. Olivera-Pastor, E. R. Losilla, M. A. Aranda, L. Leon-Reina, M. Papadaki, A. C. McKinlay, R. E. Morris, K. D. Demadis and A. Cabeza, *Dalton Trans.*, 2012, **41**, 4045-4051.
13. J. Perdew, K. Burke and M. Ernzerhof, *Errata:(1997) Phys. Rev. Lett.*, 1996, **78**, 1396.
14. P. Giannozzi, S. Baroni, N. Bonini, M. Calandra, R. Car, C. Cavazzoni, D. Ceresoli, G. L. Chiarotti, M. Cococcioni and I. Dabo, *J. Phys.: Condens. Matter*, 2009, **21**, 395502.